Accepted Manuscript

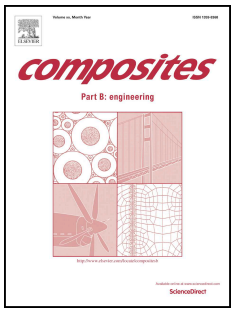

Flexural response of polypropylene/E-glass fibre reinforced unidirectional composites

Michael I. Okereke

PII: S1359-8368(16)00008-1

DOI: 10.1016/j.compositesb.2016.01.007

Reference: JCOMB 3962

To appear in: *Composites Part B*

Received Date: 23 November 2015

Revised Date: 5 January 2016

Accepted Date: 7 January 2016

Please cite this article as: Okereke MI, Flexural response of polypropylene/E-glass fibre reinforced unidirectional composites, *Composites Part B* (2016), doi: 10.1016/j.compositesb.2016.01.007.

→→→ REVISED VERSION OF MANUSCRIPT JCOMB-S-15-02629 ←←←

Flexural response of polypropylene/E-glass fibre reinforced unidirectional composites.

Michael I. Okereke*

Department of Engineering Science, University of Greenwich, Kent, United Kingdom

Abstract

This paper presents a study of the flexural response of continuous E-glass fibre reinforced polypropylene composites. Experiments were designed to investigate monotonic and cyclic flexural response using three point bending test for laminates with different angle-ply and cross-ply arrangements. Results show that the monotonic and cyclic flexural response of the composites are influenced by the plastic deformation of the matrix. The study observed that increasing numbers of cyclic loads led to significant energy dissipation, stiffness reduction and micro-damage accumulation within the composite and especially at the matrix-fibre interface. Significant energy dissipation and damage were observed to dominate the first load-unload cycle. With subsequent cycles, the magnitude of energy dissipation and global damage reduces to a threshold value which is cycle independent. This study has also developed a phenomenological model to predict the dependence of energy dissipation with number of cycles. The experimental data generated here will be useful in the development of holistic macroscale constitutive models and finite element studies of the chosen test composite.

Keywords: A. Polymer Matrix Composites, A. Plytron™, B. Three Point Bending, B. Cyclic Flexural Response

1. Introduction

In automotive and aerospace industries, the use of thermoplastics as matrix systems of fibre reinforced composites has continued to grow steadily. This is largely due to the materials' recyclability and ability to be processed rapidly. Higher strength-to-weight ratios, better chemical and impact resistance, improved fracture toughness over thermosets and enhanced fatigue strength are some other reasons why thermoplastic composites are becoming the material of choice for replacing traditional materials as steel, aluminum, wood, etc

*Corresponding Address: Department of Engineering Science, University of Greenwich, Medway Campus, Kent, ME4 4TB, United Kingdom Phone: +44 (0) 1634 88 3580 Fax: +44 (0) 1634 88 3153.

Email address: m.i.okereke@gre.ac.uk (Michael I. Okereke)

[1–4]. One particularly promising type of thermoplastic composites is cost-effective, continuous E-glass fibre reinforced polypropylene-matrix composites. These have potential as thermoformable automotive body parts [5, 6], and have attracted attention for example as possible components of composite integral body armours [7, 8], and of fibre-metal laminate sandwich structures designed for ballistic protection [9–11].

Although the use of thermoplastic composites is growing steadily, its application in structural components is inhibited by limited set of reliable experimental data about their mechanical response, especially the cyclic flexural response [12, 13]. Bending collapse of vehicles is a dominant failure mode experienced during oblique or side collisions of vehicles hence the interest in them in this paper [14]. In order to encourage the widespread adoption of thermoplastic matrix composites in different engineering applications, it is essential to widen the current understanding of their mechanical response. This demands research on both experimental investigations and numerical modelling of these composites. This work aims to generate experimental data on monotonic and cyclic flexural response of a continuous E-glass fibre reinforced polypropylene matrix composites marketed by the trade name Plytron™ [15, 16]. The interest in Plytron™ stems from the fact that it is widely used in automotive parts and has an unusually high volume fraction of matrix (i.e. 65%) compared with other thermoplastic composites.

A few authors have carried out experiments on polypropylene-based composites and such studies were focussed on the effect of processing histories on the mechanical performance of the test materials. Al-Zubaidy and co-workers [17] investigated the tensile and shear properties of orthotropic glass-polypropylene composites made under different processing conditions and found that crossply laminates had excellent tensile and shear properties with interlaminar shear strength (ILSS) being 2.5 times the ILSS of other thermoplastics composites made using the same processing history. Al-Zubaidys work also showed that Plytron™ had comparatively higher fracture toughness compared to similar composites and this was attributed to the high coupling between the fibre and the matrix components.

Data obtained from impact studies of commingled E-glass fibre polypropylene composites by Santulli and co-workers [18] were compared with those of Plytron™ and the authors reported better mechanical properties of Plytron™ than similar polypropylene-based composites. In particular, the flexural response of Plytron™ was comparable to the properties of the more aligned 4:1 weave Twintex™ composite. This observation was attributed to both the non-crimped form of the fibre reinforcement as well as improved impregnation achieved in Plytron™ composites. These excellent properties of make Plytron™ an interesting material to study.

As well as Al-Zubaidy's [17] and Santulli's [18] works, another study by Rijsdijk and co-workers [19] assessed the role of interphase modification on the mechanical response of polypropylene-based composites. The work concluded that any modifications affected significantly those composite properties that depend on the interphase, like transverse, shear and compressive strength. Thomason and colleagues [20, 21] confirmed this by carrying out a single-fibre pullout test on composites modified using different interface coatings. The flexural strength of the glass fibre/polypropylene composite was found to vary by a factor of two depending on the type of glass fibre coating used.

Most recently, Hagstrand and co-workers [22] investigated the effect of percentage void volume fraction to the mechanical behaviour of commingled E-glass fibre polypropylene-

matrix composites. They hoped that by optimizing manufacturing techniques to minimize formation of voids, composites of improved mechanical responses could be obtained. The authors found the presence of voids had negative effects on the flexural modulus and strength except surprisingly the flexural rigidity, EI which was found to increase by 2% with each 1% increase in percentage void volume fraction. It was thought that the presence of voids led to increase in dimensions of tested specimen hence increasing the moment of inertia.

Simeoli and colleagues [23] reported that changes to the interface strength of PP/E-glass fibre laminates affected their low velocity impact behaviour. By incorporating a compatibilizer, the authors found that the flexural modulus and the strength of the composite were significantly increased. The authors observed that interface failure occurred at low strains for non-compatibilizer-strengthened composites. The authors explained that the failure resulted from large energy dissipation occurring at the polymer/fibre matrix. This conclusion was confirmed using what they described as locked-in thermographic analysis of the tested specimen [24].

This short review into mechanical (especially flexural) response of PP/E-glass fibre composites highlights the sustained research interest in such composites but most significantly shows the importance of accumulating more experimental data on thermoplastic composites with dominant matrix composition as Plytron™ . The development of micromechanical and macroscale constitutive models of thermoplastic composites will benefit immensely from reliable experimental data generated through uniaxial, flexural, shear and fatigue testing of such composites. Motivated by this need, this paper presents experimental data on a series of experiments carried out with specific focus of understanding the monotonic and short cycle flexural behaviour of continuous E-glass fibre polypropylene matrix composite.

2. Test material

2.1. Plytron™ : a continuous polypropylene/E-glass fibre composite

The test material under investigation is continuous polypropylene/E-glass fibre reinforced composite. Plytron™ is the registered trademark for this continuous unidirectional glass fibre reinforced polypropylene composite made by a Swiss company called Gurit Suprem but now trades as Gurit. It is a 100% consolidated, thermoplastic composite which is commercially available as prepreg tapes of 300 mm wide, 0.25 - 0.28 mm thick and roll length of 400 m. The reinforcement is obtained with continuous unidirectional glass fibres with a weight ratio of 60-wt% (or 35-vol% fibre)[15, 16]. The matrix phase is a blend of standard polypropylene and 5% master-batch compound. The master-batch contains carbon black among other proprietary ingredients, hence giving the composite a black appearance. Plytron is commonly used in the automobile industries. Table 1 gives the manufacturer's data for typical mechanical properties of Plytron™ based on experiments performed on unidirectional and symmetric cross-ply laminates.[1]

2.2. Manufacture of test material

Composite laminates were prepared from Plytron™ prepreg tapes through compression moulding in a heated press. In preparing test specimens, plies of dimensions of 140 × 140

[1]The n in $[0_n]$ and $[(0/90)_n]_s$ within Table 1 represents the number of plies and takes values ranging from 5 - 12, whilst s represents *symmetric*.

Table 1: Physical and Mechanical Properties of Plytron™ [15, 16].

Properties	Units	$[0_n]$	$[(0/90)_n]_s$
Density, ρ	g/cm^3	1.48	1.48
Fibre Content	gew%	60	
	vol%	35	
Tensile Strength, X_t	MPa	680	360
Tensile Modulus, E_{xx}	GPa	22.5	16
Elongation at break, ϵ_f	%	2.1	2.5
Flexural Strength, $\sigma_{b,max}$	MPa	570	350
Flexural Modulus, E_b	GPa	22	16.5
Thermal Expansion Coefficient,α_T	μm/mK	7	20

mm were cut from the reel of prepreg tapes. The plies were then arranged according to a desired stacking sequence and placed inside a picture-frame mould specially designed for the moulding of test specimens. A PTFE spray was applied onto the inside lid and inside base plates of the mould to help in easy removal of the laminates after moulding. Each moulding was made under the optimal processing conditions of: (a) temperature of heated press platens: $22^o - 250^o$ C, (b) pressure applied on top and bottom of the mould: 1.5 - 2.0 MPa, (c) number of plies per laminate: 12 plies (for a laminate of thickness 3.0mm), and (d) processing cycle: 25 mins (comprising 10 mins heating up, 5 minutes dwell time and 10 mins cooling period). Typical heating and cooling rates were 15^o C/min and 20^o C/min respectively. Successive loading and unloading cycles, over 30-second intervals from start of heating, were applied to ensure that any trapped air pockets that would cause voiding were forced out. The mould was cooled from the set platen temperature to room temperature by water cooling of the heated platens.

2.3. Microscopy of test composite

The microstructure of the manufactured test material was assessed using optical and scanning electron microscopy studies. These studies were carried out to explore the nature of the interaction/bonding between the matrix and the glass fibre reinforcement and also check for the absence of voids in order to ensure the suitability of the test specimens for flexural tests. The laminates under investigation have a unidirectional layup. They were cut into specimens of dimensions of 10×10 mm^2 using a band-saw with fine blades. The specimens were mounted on Bakelite and polished for between 40-60 mins using Kemet self-adhesive cloths diamond compound of grade 6-KD-C2 and a lubricating fluid. Once satisfactory polishing was achieved, the test specimens were imaged in an Alicona Infinite Focus profilometer set in 2D imaging mode. Micrographs were obtained in the through-thickness section of the test materials. This assessment reveals that the microstructure of Plytron™ consists of clearly defined regions of matrix-rich and fibre-rich zones (see *Figures 1(a) to 1(c)*) - typical of laminated composites. Scanning electron microscopy was used to obtain micrographs demonstrating excellent bonding between the matrix and fibre as shown in *Figure 1(d)*. This confirms that the laminate making process achieved high level

of consolidation. In all the assessed micrographs, voiding was very minimal.

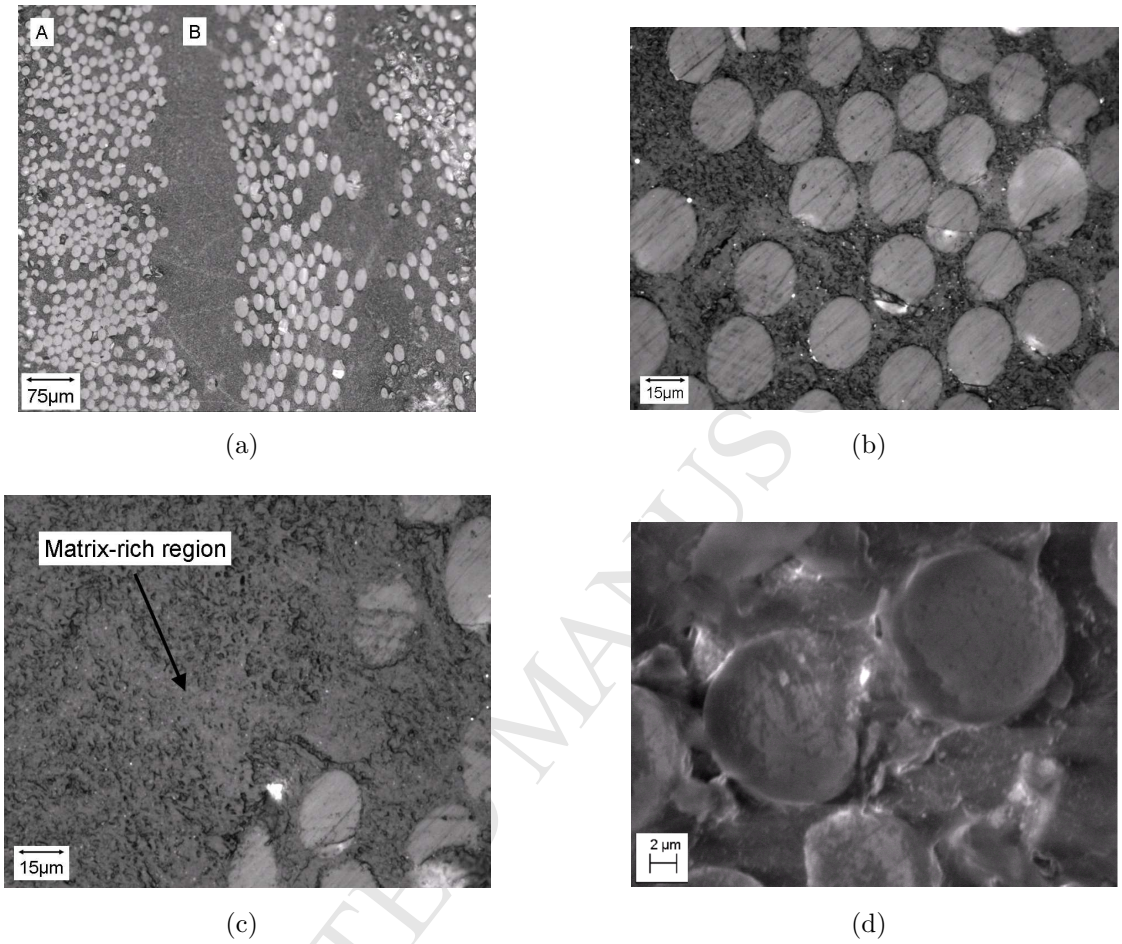

Figure 1: Optical micrographs of a typical test specimen showing: (a) banded arrangement of fibre (grey circles) within the matrix (black region); (b) random arrangement of fibres within fibre-rich zone (A); and (c) limited distribution of fibres within matrix-rich zone (B); as well as (d) zoomed-in view of two individual fibres: showing good fibre-matrix consolidation, and absence of voids.

3. Experimental test setup and specimen design

Compression moulded laminates with different fibre orientations were cut into beam specimens and tested by three-point bending test. Symmetric laminates of stacking sequences were studied where $\theta = 0^o, 15^o, 30^o, 45^o, 60^o, 75^o$, and 90^o and $n = 5$. Also, cross-ply specimens of stacking sequence $[(0/90)_5]_s$ were also tested. *Figure 2* shows the geometry of three point bending test specimens.

According to the ISO 14125:1998 test standard for flexural test of fibre-reinforced plastic composites, the dimension of the test specimen was chosen as $70 \times 20 \times 2.8$ mm^3. All tests were carried out using an Instron Series IX Automated Materials Testing System 4204. A three-point bending test rig, shown in *Figure 3*, was fitted to the Instron machine such that when tensile load is applied on the end supports of the test specimen, the specimen responds in bending around a mid-span fulcrum support of radius 2.5 mm. Flexural forces

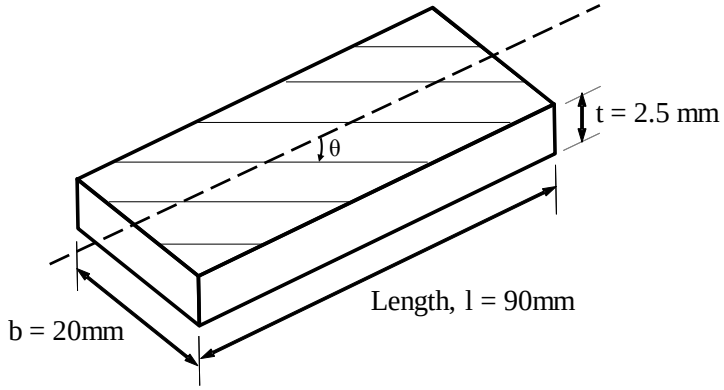

Figure 2: Design of a three-point bending test specimen.

were measured using a 5 kN load cell while the deflection of the beam was measured by crosshead displacement. Tests were carried at crosshead speed of 5 mm/min.

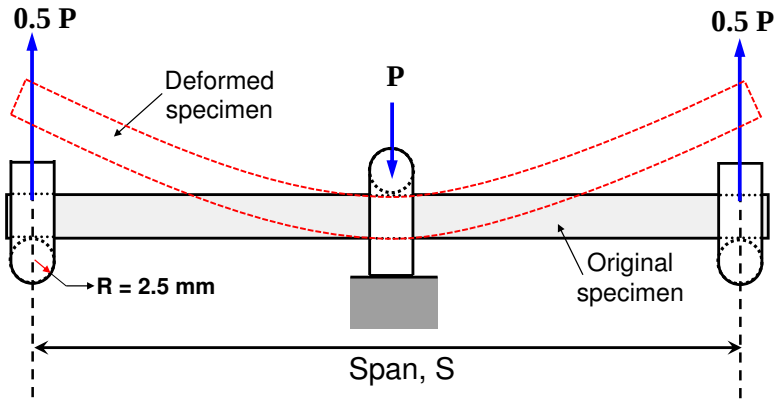

Figure 3: Schematic representation of a three-point bending test rig highlighting the test specimen and loading arrangement that enforces the bending response of the test material.

4. Test Results

4.1. Monotonic flexural tests

The flexural response of Plytron™ is presented in plots of Force, F [N] against mid-span deflection of the beam, δ [mm]. The maximum flexural force, F_{max} is identified as the peak force on the flexural force-deflection plot. *Figures 4(a) - 4(h)* show plots of flexural responses of Plytron™ laminates for fibre orientations from 0^o to 90^o. The 0^o test specimens refer to unidirectional composites where the fibre-axis aligns with the longitudinal neutral axis of the test specimen. The plot for the 0^o laminates was dominated by the linear elasticity of the fibre, as shown in *Figure 4(a)*. Similarly, the flexural response of 90^o test specimens was determined transverse to the fibre's longitudinal direction. In this later case, the flexural response was dominated by the nonlinear viscoelasticity of the matrix, as shown in *Figure 4(f)*. Also, three-point bending tests were carried out on cross-ply laminates and the result is shown in *Figure 4(g)*. The comparison showing the full range of the monotonic flexural

response of this class of composite is shown in *Figure 4(h)* which shows the dependence of the composite flexural response with fibre orientations. These results show, as expected that the flexural response of the thermoplastic matrix composite was linear elastic till yield for fibre-dominated directions (i.e. for fibre orientation, $\theta = 0^0, 15^0$ and $[(0/90)_5]_s$) while for the other fibre orientations, the plasticity of the matrix dominated the flexural response.

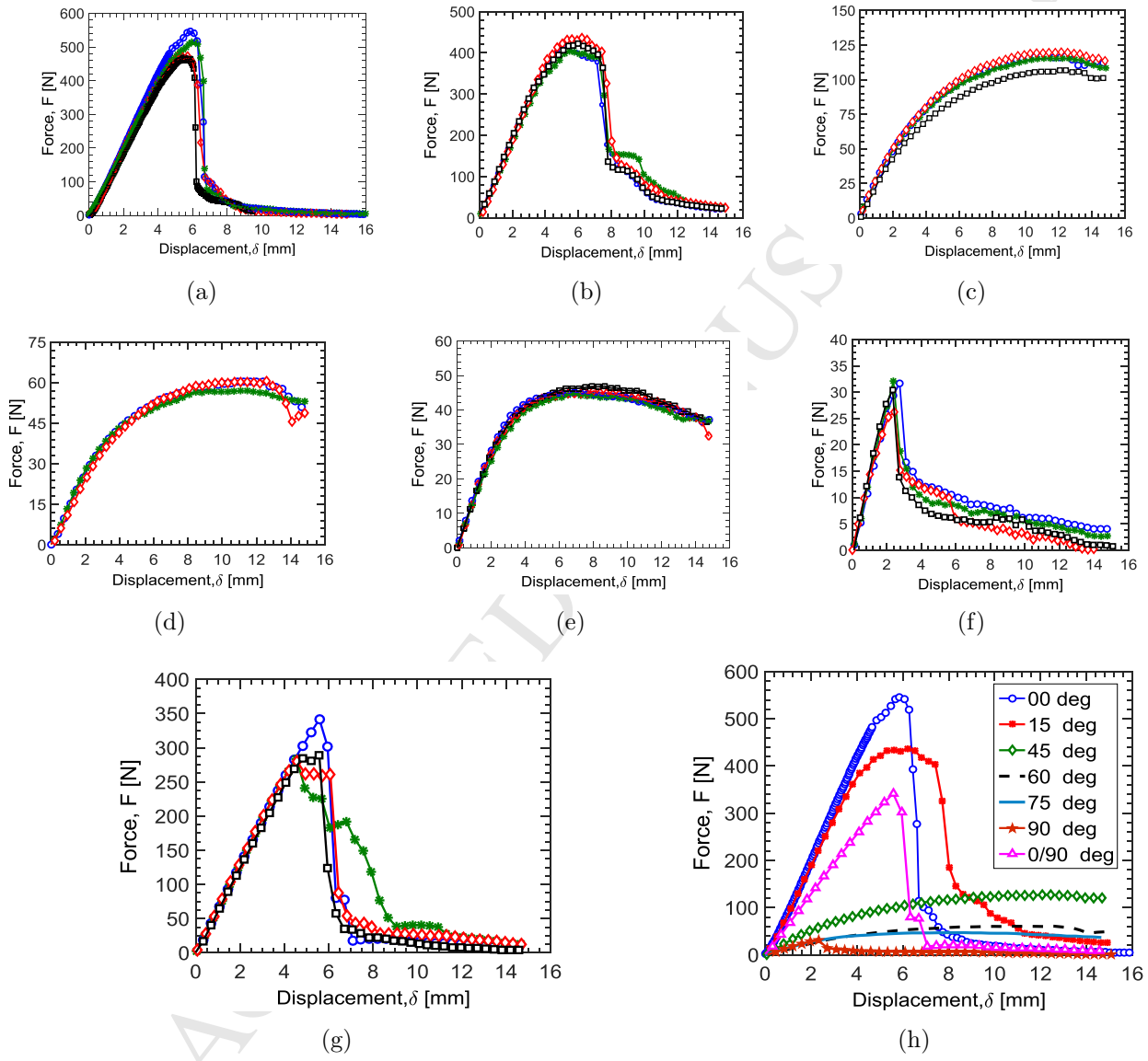

Figure 4: Monotonic flexural response of Plytron™ laminates for the following stacking sequences: (a) $[0_{10}]$, (b) $[(\pm 15)_5]_s$, (c) $[(\pm 45)_5]_s$, (d) $[(\pm 60)_5]_s$, (e) $[(\pm 75)_5]_s$, (f) $[90_{10}]$, (g) $[(0/90)_5]_s$, (h) comparison of all fibre orientations.

4.2. Short cycle flexural tests

The aim here was to investigate the flexural response of Plytron™ under short cycle loading. Similar specimen design and test rig used in the previous section were used in these tests. The test specimens were tested in the Instron Machine in displacement-control mode.

A limiting deflection, δ_{limit} (herein referred to as *cyclic deflection limit* (CDL)), was chosen such that deflection does not exceed 80% of the flexural peak load (i.e. $\delta_{limit} \leq 80\%$) for each laminate under consideration. This δ_{limit} also ensures that the loading regime exceeds the elastic limit of the laminates but not approach the unstable region of onset of failure. As a result, it was possible to investigate as reported in *Section 5.4*, the accumulation of microscopic damage until eventual failure.

All test specimens were subject to cyclic loads of up to 5 cycles and typical force-deflection plots for a cross-ply and four angle-ply laminates are shown in *Figure 5(a)* - *5(e)*. Only 5 cycles were chosen as this study was aimed at short cycle fatigue. Traditionally, during fatigue tests, tests specimens are subjected to hundreds of thousands of cycles, in order to assess the cyclic response of the test material. For the purpose of this work, it has been observed, and reported later in *Section 5.3* that after the first three - five cycles, the composite experiences a cycle independent energy dissipation which is the same irrespective of increasing number of cycles. As a result, this work has focussed on the short cycle fatigue of the test composite - in the region within which significant changes in the mechanical response of the composite - is observed.

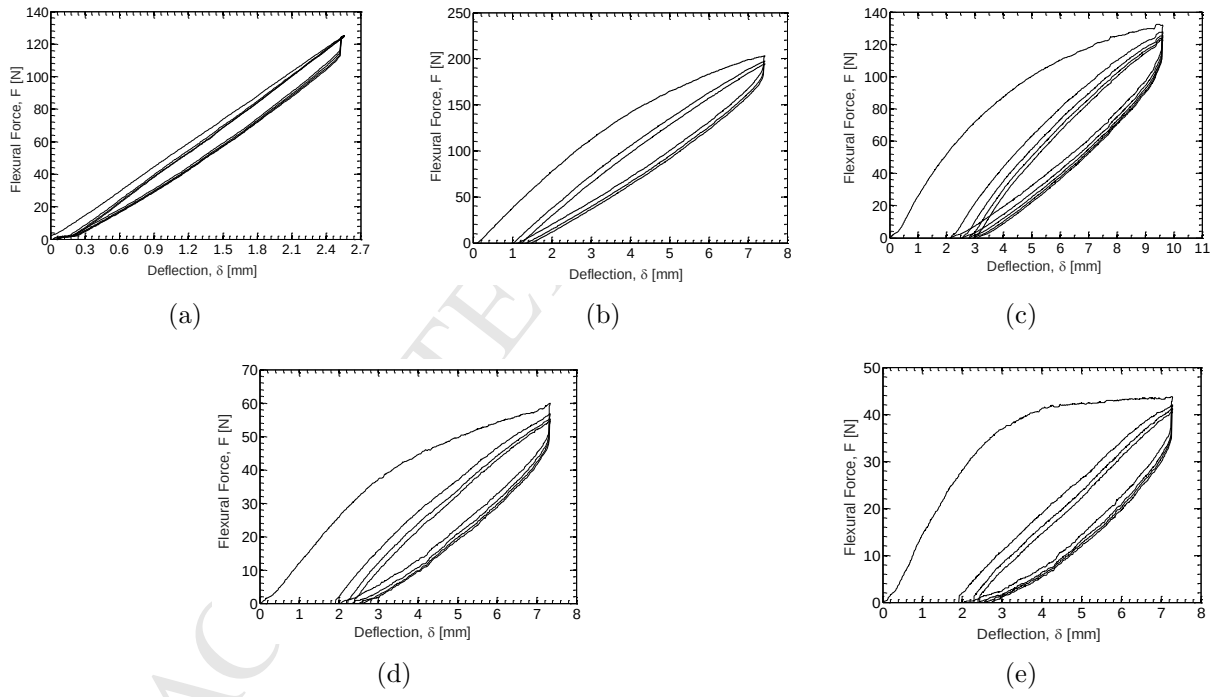

Figure 5: Short cycle flexural response of Plytron™ laminates for the following stacking sequences: (a) cross-ply $[(0/90)_5]_s$; angle-plies: (b) $[(\pm 30)_5]_s$, (c) $[(\pm 45)_5]_s$, (d) $[(\pm 60)_5]_s$, and (e) $[(\pm 75)_5]_s$ laminates.

5. Discussions

5.1. The mechanics of the composite's flexural response

At very small deflections, $\delta \ll t$ where t = thickness, the principles of classical lamination theory [25, 26] can be applied to the analysis of the linear elastic flexural response of

the symmetric laminates tested here. Consider a simply supported rectangular plate of dimensions: length, L, width, b and thickness, t subjected to bending. The moment-curvature relationship [25] of a laminated composite plate is:

$$\begin{bmatrix} M_x(t) \\ M_y(t) \\ M_{xy}(t) \end{bmatrix} = \begin{bmatrix} D_{11}(t) & D_{12}(t) & D_{16}(t) \\ D_{12}(t) & D_{22}(t) & D_{26}(t) \\ D_{16}(t) & D_{26}(t) & D_{66}(t) \end{bmatrix} \begin{bmatrix} \kappa_x(t) \\ \kappa_y(t) \\ \kappa_{xy}(t) \end{bmatrix}. \tag{1}$$

Here, $M_x(t)$ is a rate-dependent bending moment per unit width of the beam about the plane containing the bar axis; $D_{ij}(t)$ is rate-dependent laminate bending stiffness, for $i, j = 1, 2, 6$ and $\kappa_x(t)$ is the resulting rate-dependent curvature about the x-axis. For ease of writing, the rate-dependence is assumed and not explicitly written, hence $M_x(t)$ is written as simply M_x, as well as flexural stress, $\sigma(t)$ becomes σ. In a pure bending test, $\kappa_y = \kappa_{xy} = 0$. Therefore, the moment-curvature expression - based on *Equation 1* - for analysing the three-point bending tests becomes:

$$M_x = \kappa_x D_{11} \qquad \Rightarrow \qquad M = b\kappa_x D_{11} = \frac{bD_{11}}{\rho_x}, \tag{2}$$

where $b =$ width of beam, $M =$ total bending moment, and radius of curvature, $\rho_x = \kappa_x^{-1}$. For a simply supported composite beam of span, L subjected to a three-point bending by a concentrated force, F - imposed on the middle of the beam, the expression of the force per unit deflection is:

$$\frac{F}{\delta} = \frac{48EI}{L^3} \qquad \Rightarrow \qquad EI = \frac{L^3}{48}\left(\frac{F}{\delta}\right) = D_{11}. \tag{3}$$

According to simple beam theory, $M_x = \kappa_x EI_x$ which implies that the expression for the D_{11} element of the bending stiffness matrix, $\mathbf{D}$ of the composite becomes *equation 3*. The expressions for calculating the flexural strength, σ_{max} and flexural modulus, E_f of the Plytron™ laminates are given in *Equation 4* . For calculating the strength and flexural modulus of the test composite, the x-axis moment of inertia for a rectangular cross-section beam is $I_x = \frac{bt^3}{12}$ and the following equation was used:

$$\text{Strength}: \quad \sigma_{max} = \frac{3PL}{2bt^2}, \qquad \text{and} \qquad \text{Flexural Modulus}: \quad E_f = \frac{1}{4b}\left(\frac{L}{t}\right)^3 \frac{F}{\delta}. \tag{4}$$

A MATLAB script called *LamPower* was created based on the principles of the commonly used classical lamination theories[25] namely: *rule of mixtures*, *Halpin-Tsai equations*, Spencer's *square array model* as well as *simplified micromechanics equations* of Chamis[27]. Also, the much recently published closed-form micromechanics equations herein called Morais' *self-consistent model*[28] was also implemented within *LamPower*. The script was used to generate the **D**-matrix for a given laminated stacking sequence, having specified the elastic properties and volume fractions of the constituents as well as the ply size and the stacking sequence of the laminates. The output from *LamPower* was used to derive predicted flexural modulus used in the next section.

5.2. Comparison of experiments with laminate theory predictions

The objective here is to compare experimentally determined laminate bending stiffness of Plytron™ with predictions based on the classical laminate theory established in *Section 5.1* above. In the expression for D_{11} in *Equation 3*, the term $\frac{F}{\delta}$ (unit = [N/mm]) is the slope (for $\delta \ll t$) of the force-deflection plots of *Figure 4*. Using the deflection of $\delta = 0.5$ mm and the Modulus expression of *Equation 4*, *Figure 4* data were used to determine the laminate bending stiffness for all six fibre orientations. The properties of the fibre and matrix constituents, given in *Table 2*, were used to determine the D_{11} term of the **D**-matrix. Predicted values of the bending stiffness were determined using the *LamPower* implementation of the classical laminate theory.

Table 2: Typical room temperature properties of E-glass fibre reinforcement and isotropic semicrystalline polypropylene matrix used in Plytron™.

Property	**Fibre**	**Matrix**	**Units**
Density, ρ	2600	900	kg/m^3
Young's Modulus, E	73	1.308	GPa
Tensile Strength, X	2250	40	MPa
Shear Modulus, G	31	0.46	GPa

In determining the predicted values, the size of each laminate ply was found to be 0.25 ± 0.002 mm. This was calculated from the plot of number of plies, N used per laminate against thickness, t of the laminate. Six mouldings of different thicknesses ranging from $t = 2.5$ mm to $t = 10$ mm were used. The ply size: 0.25 ± 0.002 mm, was determined by substituting N = 1 (for one ply) into the linear function of plot of number of plies per laminate versus laminate thickness. *Figure 6* shows the comparison of the experimental and predicted variation of the laminate flexural modulus, E_f with ply orientation, θ. The results in *Figure 6* show a good agreement, within experimental error, between the experimental and predicted E_f values for all fibre orientations based on the Morais *self-consistent model* [28]. According to this result, the Spencer's *square array model*[25] and Chamis' *simplified micromechanics model*[27] established upper and lower bounds to the E_f values.

5.3. Quantifying the energy dissipation for cyclic flexural response

The stress-strain cyclic profile following a uniaxial fatigue test gives a measure of the stiffness degradation or energy dissipation experienced by a test material. Similarly, the force-deflection plot of a three-point bending tests as reported here can give information of degradation of stiffness or energy dissipation as the uniaxial tests [29–31]. In order to quantify the cyclic flexural response, let us define an *energy dissipation factor,* ζ_d as in *Equation 5*:

$$\text{Energy dissipation factor,} \quad \zeta_d = 1 - \frac{E_{unloading}}{E_{loading}}, \tag{5}$$

where $E_{loading}$ is the strain energy of the loading curve segment whilst $E_{unloading}$ is the strain energy of the unloading curve segment. These strain energies were determined as the

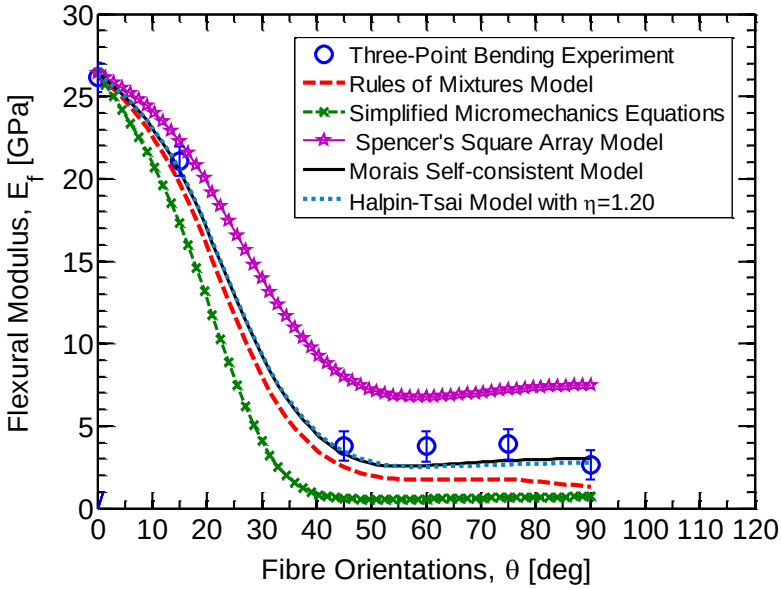

Figure 6: Comparison of experimental and predicted flexural modulus, E_f. The prediction was based on selected composite lamination theories. *Note: The error bars was determined by calculating the standard deviation of the slope of the force-displacement plots for all the tested specimens per given fibre orientation*

areas under the appropriate curve segment. The areas were calculated numerically using the trapezoidal rule. For the three-point bending test, the ζ_d parameter represents a quantitative measure the energy dissipation following successive cyclic loading of the the material[29].

Consider the cyclic flexural response of $[(\pm 45)_5)]_s$ Plytron^{TM} laminate, the test specimen was subjected to 5 cycles of flexural loading as shown in *Figure 7(a)* . The short cycle flexural response the Plytron^{TM} laminates shown in *Figure 7(b)* indicates that at the end of the unloading curve, the laminate does not return to zero deflection but there exists a residual deflection. For the first cycle of the $[(\pm 45)_5]_s$ Plytron^{TM} laminate, the residual deflection was 2.1 mm and by the fifth cycle, this has reduced 0.32 mm. Similarly, the area under the load-unload curves evolves from 504 N-mm to 147 N-mm.

It is customary to represent ζ_d as a percentage, thus providing a measure of energy dissipation between successive cycles. Using the cyclic plots of *Figure 5* and *Equation 5*, the plots of energy dissipation factor, ζ_d against number of cycles, N for both angle-ply and cross-ply laminates are shown in *Figure 8*. The plot of *Figure 8* shows that for increasing angle, θ between the fibre and the main axis of bending, the percentage energy dissipation factor, ζ_d increases. Cross-ply laminates show very small energy dissipation compared with the angle-ply laminates.

The data in *Figure 8* shows the most significant energy loss occurred between the first two cycles. For example, for the $[(\pm 75)_5]_s$ laminates, the percentage change in energy dissipation $\Delta\zeta_d = 70\% - 46\% = 24\%$ whilst for the $[(0/90)_5]_s$ laminates, $\Delta\zeta_d = 3\%$. The cyclic flexural response of the test composite indicates significant energy dissipation in those laminate arrangements that experience significant plastic deformation. Therefore, structural applications requiring significant energy absorption in the first loading cycle can be made based on the test material with the $[(\pm 45)_5]_s]$ laminate arrangement.

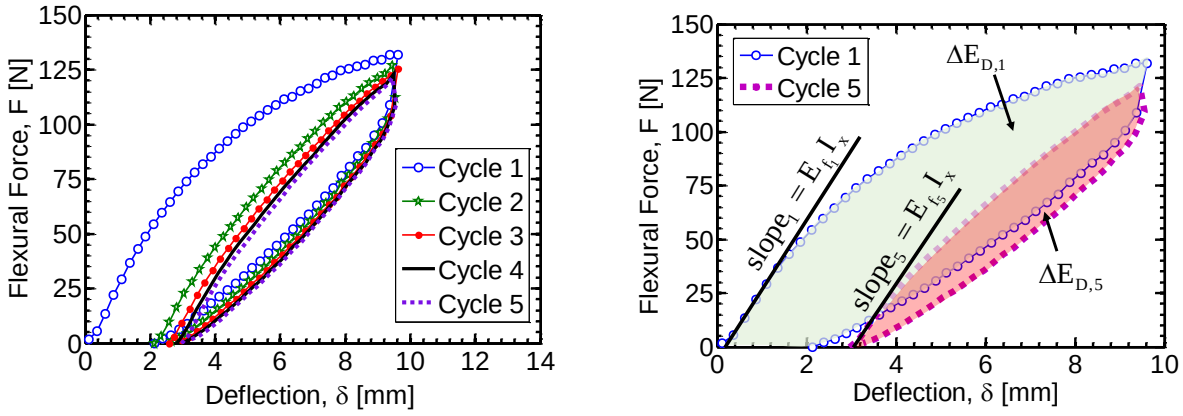

(a) (b)

Figure 7: Short cycle flexural response of the $[(\pm 45)_5]_s$ laminates for: (a) all 5 cycles and : (b) first and fifth cycles. The energy dissipation for an $n-th$ cycle ΔE_n is shown as well as the slopes for the first and fifth cycles where the tested specimen flexural modulus of $n-th$ cycle is $E_{f,n}$ and the area moment of inertia about the x-axis is I_x.

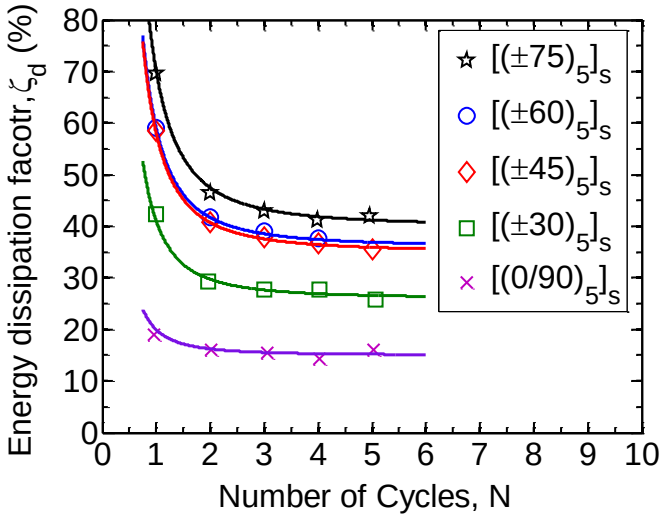

Figure 8: Plots of energy dissipation for all the tested composites. *Note: Solid trend lines indicate model predictions while markers are experimental data.*

To quantify mathematically the dependence of percentage energy dissipation factor, ζ_d with number of cycles, N, this study established that the numerical fit of the experimental data of *Figure 8* can be expressed by the power law:

$$\zeta_d = AN^b + \zeta_{d,0} \tag{6}$$

where ζ_d = energy dissipation factor, N= number of cycles, $\zeta_{d,0}$ = threshold energy dissipation factor and finally A, b are material constants. Typical values of A, b and $\zeta_{d,0}$ for the laminates arrangements tested here are shown in *Table 3*.

Equation 3 represents a phenomenological model for characterizing the short cycle flexural response of Plytron™ laminates. The A-parameter is a measure of *first-cycle percentage*

Table 3: Typical values of material constants for the energy dissipation function associated with short cycle flexural behaviour of Plytron™ laminates.

Stacking Sequence	A	b	$\zeta_{d,0}$
$[(0/90)_5]_s$	5	-2.0	15
$[(\pm30)_5]_s$	15	-2.0	26
$[(\pm45)_5]_s$	23	-2.0	35
$[(\pm60)_5]_s$	23	-2.0	36
$[(\pm75)_5]_s$	30	-2.0	40

change in energy dissipation. The A-parameter is high for laminate arrangements that show dominant plastic deformation (e.g. the $[(\pm75)_5]_s$ and $[(\pm60)_5]_n$ angle-ply laminates). The $\zeta_{d,0}$-parameter is a measure of the energy dissipation of the test material that remains constant with increasing number of cycles. Kar and co-workers [31] reported similar observation for the bending fatigue of hybrid composites.

5.4. Damage accumulation in cyclic flexural response

With increasing number of cyclic loadings, the mechanical properties of composite materials degrade progressively. The global damage caused by the cyclic flexural loading of the test composite can be measured effectively by measuring the stiffness degradation of the material [31–33]. An objective measure of this degradation is the global damage index, D which can be defined as:

$$D = \left[1 - \frac{(EI)_n}{(EI)_1} \right], \tag{7}$$

where $(EI)_n$ is the cyclic flexural rigidity after the $n-th$ cycle, and $(EI)_1$ is the flexural rigidity after the first cycle for the tested cyclic deflection level, δ_{limit}. These flexural moduli are related to a chosen δ_{limit} and should be differentiated from statically determined flexural modulus, $(EI)_0$ which is a reference value for monotonic flexural test deformed till failure of the test material. Several microscopic damage mechanisms are assumed to contribute to the D. For the thermoplastic matrix composites under investigation, these damage/failure mechanisms are usually matrix-dominated and can include: matrix cracking (or more generally inter-fibre failure), fibre-matrix debonding, ply delamination, fibre rupture and finally fibre kinking[34]. Kar and co-workers [31] observed that with subsequent cycles, the microscopic damage continues to localize especially in the matrix and matrix-interphase phases until eventual failure occurs. The final flexural rigidity at failure, $(EI)_f$ is calculated at the last loading cycle before eventual failure. This will yield a GDI value of D_f defined as global damage index at failure of the test material.

Combining *Equation 3* and the cyclic flexural data of *Figure 5*, the flexural rigidity, EI for each loading cycle was determined. These $EI's$ were then used with *Equation 7* to calculate the associated *global damage index, D* for the last $n-th$ cycle (representative of accumulated damage). The plot of the percentage *global damage index, D* against the tested laminate arrangements is shown in *Figure 9*.

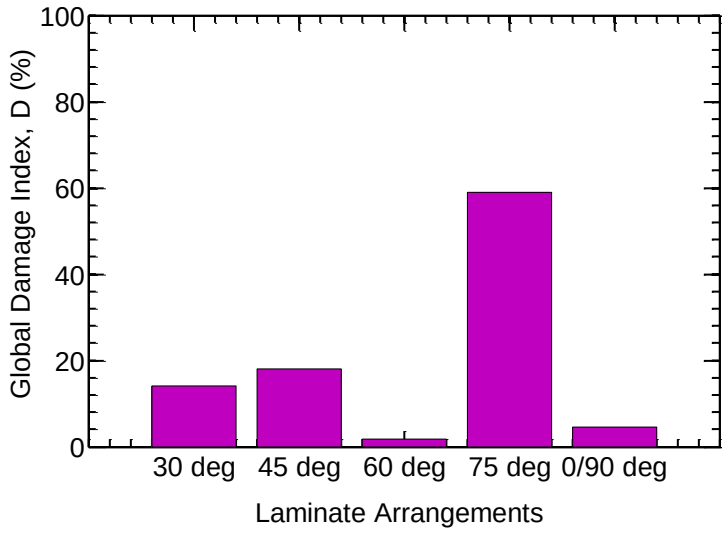

Figure 9: Histogram of global damage index, D for all laminate arrangements. *Note: D is expressed here as a percentage, for easy interpretation of the extent of damage.*

The result shown in *Figure 9* shows that damage accumulation was the most in the $[(\pm 75)_5]_s$ laminates and the least in the $[(\pm 60)_5]_s$ laminates. The high damage accumulation seen in the $[(\pm 75)_5]_s$ indicates that for same cyclic deflection level (CDL), δ_{limit}, more microscopic damage occur than in say the $[(\pm 60)_5]_s$ laminates. Gamstedt and Talreja [35] investigated the fatigue damage mechanisms in unidirectional carbon-reinforced composites with thermoset and thermoplastic matrices. The study showed the fatigue damage is a cumulative effect of microscopic damage of the matrix and was particularly pronounced in the thermoplastic (PEEK) matrix composites. These microscopic damages comprise of widespread propagating debonds and matrix cracks. The authors did not assess the effect of changing fibre orientation on the evolution of these microscopic damage. This evidence, amongst several others, support the claim in this work that the observed damage accumulation as shown in *Figure 9* is a consequence of progressively accumulating microscopic failure mechanisms

6. Conclusions

The paper reports on the monotonic and cyclic flexural response of continuous E-glass fibre reinforced polypropylene composites (marketed as Plytron^{TM}). By changing the orientation, θ of the fibre to the main bending axis, the flexural response of the laminates changed from a linear elasticity dominant response until damage to a plasticity-dominant response. Therefore, the effect of the matrix is significant in understanding the flexural response of this type of thermoplastic matrix composite. Experimentally-derived flexural modulus of all tested laminates were found to agree with predictions of the same based on classical lamination theories.

Similarly, short cycle flexural response of Plytron^{TM} was investigated for five stacking sequences of the laminates. The study also developed a phenomenological model that describes the dependence of energy dissipation with number of cycles. The study observed

that for all tested laminates, the largest energy dissipation occurred after the first cycle and thereafter, the energy dissipation converges quickly to a cycle-independent energy dissipation value which is a material constant. This cycle-independent energy dissipation is thought to be a saturated damaged state (or maximum energy-dissipation) within the test material. The size of initial and saturated energy dissipation increases as the angle of fibre orientation relative to the main bending axis increases too.

In conclusion, the flexural response of continuous E-glass fibre reinforced polypropylene composites has been studied experimentally. It is concluded here that the plastic deformation of the matrix contributes significantly to the flexural response. To encourage wider application of this type of material in structural designs, it is imperative that a constitutive model need to be developed. On evidence from this work, such model development must consider the contribution of a robust matrix model towards the accurate prediction of the mechanical response of Plytron^{TM} . The experimental data presented here and the associated phenomenological models will help in the micro-mechanical modelling for the class of thermoplastic matrix composites as Plytron^{TM} with a comparatively higher matrix volume fraction.

References

[1] Offringa, A.R.. Thermoplastic compositesrapid processing applications. Composites Part A: Applied Science and Manufacturing 1996;27(4):329–336.

[2] Parlevliet, P.P., Bersee, H.E., Beukers, A.. Residual stresses in thermoplastic compositesa study of the literaturepart i: Formation of residual stresses. Composites Part A: Applied Science and Manufacturing 2006;37(11):1847 – 1857. doi:\bibinfo{doi}{http://dx.doi.org/10.1016/j.compositesa.2005.12.025}. URL http://www.sciencedirect.com/science/article/pii/S1359835X06000145.

[3] Stewart, R.. Thermoplastic compositesrecyclable and fast to process. Reinforced Plastics 2011;55(3):22–28.

[4] Sorrentino, L., Simeoli, G., Iannace, S., Russo, P.. Mechanical performance optimization through interface strength gradation in pp/glass fibre reinforced composites. Composites Part B: Engineering 2015;76:201 – 208. doi:\bibinfo{doi}{http://dx.doi.org/10.1016/j.compositesb.2015.02.026}. URL http://www.sciencedirect.com/science/article/pii/S1359836815001122.

[5] Holbery, J., Houston, D.. Natural-fiber-reinforced polymer composites in automotive applications. The Journal of The Minerals, Metals and Materials Society 2006;58(11):80–86. doi:\bibinfo{doi}{10.1007/s11837-006-0234-2}. URL http://dx.doi.org/10.1007/s11837-006-0234-2.

[6] Ashori, A.. Woodplastic composites as promising green-composites for automotive industries! Bioresource Technology 2008;99(11):4661 – 4667. doi:\bibinfo{doi}{http://dx.doi.org/10.1016/j.biortech.2007.09.043}. Exploring Horizons in Biotechnology: A Global Venture; URL http://www.sciencedirect.com/science/article/pii/S0960852407007560.

[7] Fink, B.K.. Performance metrics for composite integral armor. Journal of Thermoplastic Composite Materials 2000;13(5):417–431. doi:\bibinfo{doi}{10.1106/FR0L-T33W-JPD0-VFH3}. http://jtc.sagepub.com/content/13/5/417.full.pdf+html; URL http://jtc.sagepub.com/content/13/5/417.abstract.

[8] Savage, G., Tacon, K., Welsh, I.. Composite armour materials. 1993. EP Patent 0,417,929; URL https://www.google.com/patents/EP0417929B1?cl=en.

[9] Villanueva, G.R., Cantwell, W.. The high velocity impact response of composite and fml-reinforced sandwich structures. Composites Science and Technology 2004;64(1):35 – 54. doi:\bibinfo{doi}{http://dx.doi.org/10.1016/S0266-3538(03)00197-0}. URL http://www.sciencedirect.com/science/article/pii/S0266353803001970.

[10] Abdullah, M., Cantwell, W.. The impact resistance of polypropylene-based fibremetal laminates. Composites Science and Technology 2006;66(1112):1682 – 1693. doi:\bibinfo{doi}{http://dx.doi.org/10.1016/j.compscitech.2005.11.008}. URL http://www.sciencedirect.com/science/article/pii/S0266353805004203.

[11] Carrillo, J., Cantwell, W.. Mechanical properties of a novel fibermetal laminate based on a polypropylene composite. Mechanics of Materials 2009;41(7):828 – 838. doi:\bibinfo{doi}{http://dx.doi.org/10.1016/j.mechmat.2009.03.002}. URL http://www.sciencedirect.com/science/article/pii/S0167663609000593.

[12] Jen, M.H., Lee, C.H.. Strength and life in thermoplastic composite laminates under static and fatigue loads. part i: Experimental. International Journal of Fatigue 1998;20(9):605 – 615. doi:\bibinfo{doi}{http://dx.doi.org/10.1016/S0142-1123(98)00029-2}. URL http://www.sciencedirect.com/science/article/pii/S0142112398000292.

[13] Hwang, J.S., Choi, T.G., Lee, D., Lyu, M.Y., Lee, D.G., Yang, D.Y.. Dynamic and static characteristics of polypropylene pyramidal kagome structures. Composite Structures 2015;131:17 – 24. doi:\bibinfo{doi}{http://dx.doi.org/10.1016/j.compstruct.2015.04.065}. URL http://www.sciencedirect.com/science/article/pii/S0263822315003608.

[14] Eksi, S., Genel, K.. Bending response of hybrid composite tubular beams. Thin-Walled Structures 2013;73:329 – 336. doi:\bibinfo{doi}{http://dx.doi.org/10.1016/j.tws.2013.09.001}. URL http://www.sciencedirect.com/science/article/pii/S0263823113002164.

[15] GuritSuprem, . Material safety data sheet - plytron: According to ec directive 91/155/eec. Tech. Rep.; GuritSuprem; 2004.

[16] GuritSuprem, . Plytron - product description, properties and applications - a technical report. Tech. Rep.; Gurit Composite Technologies; 2005.

[17] Al-Zubaidy, M., Chan, J., Gibson, A., Toll, S.. Properties of orthotropic glasspolypropylene

composites manufactured by weaving of prepregtapes and other routes. Plastics, Rubber and Composites 2000;29(10):520–526. doi:\bibinfo{doi}{10.1179/146580100101540725}. http://dx.doi.org/10.1179/146580100101540725; URL http://dx.doi.org/10.1179/146580100101540725.

[18] Santulli, C., Brooks, R., Long, A.C., Warrior, N.A., Rudd, C.D.. Impact properties of compression moulded commingled e-glasspolypropylene composites. Plastics, Rubber and Composites 2002;31(6):270–277. doi:\bibinfo{doi}{10.1179/146580102225004983}. http://dx.doi.org/10.1179/146580102225004983; URL http://dx.doi.org/10.1179/146580102225004983.

[19] Rijsdijk, H., Contant, M., Peijs, A.. Special issue microphenomena in advanced composites continuous-glass-fibre-reinforced polypropylene composites: I. influence of maleic-anhydride-modified polypropylene on mechanical properties. Composites Science and Technology 1993;48(1):161 – 172. doi:\bibinfo{doi}{http://dx.doi.org/10.1016/0266-3538(93)90132-Z}. URL http://www.sciencedirect.com/science/article/pii/026635389390132Z.

[20] Thomason, J., Schoolenberg, G.. An investigation of glass fibre/polypropylene interface strength and its effect on composite properties. Composites 1994;25(3):197 – 203. doi:\bibinfo{doi}{http://dx.doi.org/10.1016/0010-4361(94)90017-5}. URL http://www.sciencedirect.com/science/article/pii/0010436194900175.

[21] Yang, L., Thomason, J.. Interface strength in glass fibrepolypropylene measured using the fibre pull-out and microbond methods. Composites Part A: Applied Science and Manufacturing 2010;41(9):1077 – 1083. doi:\bibinfo{doi}{http://dx.doi.org/10.1016/j.compositesa.2009.10.005}. Special Issue on 10th Deformation and Fracture of Composites Conference: Interfacial interactions in composites and other applications; URL http://www.sciencedirect.com/science/article/pii/S1359835X09003157.

[22] Hagstrand, P.O., Bonjour, F., Mnson, J.A.. The influence of void content on the structural flexural performance of unidirectional glass fibre reinforced polypropylene composites. Composites Part A: Applied Science and Manufacturing 2005;36(5):705 – 714. doi:\bibinfo{doi}{http://dx.doi.org/10.1016/j.compositesa.2004.03.007}. URL http://www.sciencedirect.com/science/article/pii/S1359835X04000740.

[23] Simeoli, G., Acierno, D., Meola, C., Sorrentino, L., Iannace, S., Russo, P.. The role of interface strength on the low velocity impact behaviour of pp/glass fibre laminates. Composites Part B: Engineering 2014;62:88 – 96. doi:\bibinfo{doi}{http://dx.doi.org/10.1016/j.compositesb.2014.02.018}. URL http://www.sciencedirect.com/science/article/pii/S135983681400095X.

[24] Russo, P., Acierno, D., Simeoli, G., Iannace, S., Sorrentino, L.. Flexural and impact response of woven glass fiber fabric/polypropylene composites. Composites Part B: Engineering 2013;54:415 – 421. doi:\bibinfo{doi}{http://dx.doi.org/10.1016/j.compositesb.2013.06.016}. URL http://www.sciencedirect.com/science/article/pii/S1359836813003272.

[25] Gibson, R.. Principles of Composite Material Mechanics, Third Edition. Mechanical Engineering; Taylor & Francis; 2011. ISBN 9781439850053. URL https://books.google.co.uk/books?id=vxg9Z4aJ36MC.

[26] Jones, R.. Mechanics Of Composite Materials. Materials Science and Engineering Series; Taylor & Francis; 1998. ISBN 9781560327127. URL https://books.google.co.uk/books?id=oMph2kNG3yAC.

[27] Chamis, C.C.. Simplified composite micromechanics for predicting microstresses. Journal of Reinforced Plastics and Composites 1987;6(3):268–289. doi:\bibinfo{doi}{10.1177/073168448700600305}. http://jrp.sagepub.com/content/6/3/268.full.pdf+html; URL http://jrp.sagepub.com/content/6/3/268.abstract.

[28] de Morais, A.B.. Transverse moduli of continuous-fibre-reinforced polymers. Composites Science and Technology 2000;60(7):997 – 1002. doi:\bibinfo{doi}{http://dx.doi.org/10.1016/S0266-3538(99)00195-5}. URL http://www.sciencedirect.com/science/article/pii/S0266353899001955.

[29] Paepegem, W.V., Geyter, K.D., Vanhooymissen, P., Degrieck, J.. Effect of friction on the hysteresis loops from three-point bending fatigue tests of fibre-reinforced composites. Composite Structures 2006;72(2):212 – 217. doi:\bibinfo{doi}{http://dx.doi.org/10.1016/j.compstruct.2004.11.006}. URL http://www.sciencedirect.com/science/article/pii/S0263822304003794.

[30] Sakin, R., rfan Ay, , Yaman, R.. An investigation of bending fatigue behavior for glass-fiber reinforced polyester composite materials. Materials & Design 2008;29(1):212 – 217. doi:\bibinfo{doi}{http://dx.doi.org/10.1016/j.matdes.2006.11.006}. URL http://www.sciencedirect.com/science/article/pii/S0261306906003451.

[31] Kar, N., Barjasteh, E., Hu, Y., Nutt, S.. Bending fatigue of hybrid composite rods. Composites Part A: Applied Science and Manufacturing 2011;42(3):328 – 336. doi:\bibinfo{doi}{http://dx.doi.org/10.1016/j.compositesa.2010.12.012}. URL http://www.sciencedirect.com/science/article/pii/S1359835X10003283.

[32] Mao, H., Mahadevan, S.. Fatigue damage modelling of composite materials. Composite Structures 2002;58(4):405 – 410. doi:\bibinfo{doi}{http://dx.doi.org/10.1016/S0263-8223(02)00126-5}. URL http://www.sciencedirect.com/science/article/pii/S0263822302001265.

[33] Wu, F., Yao, W.. A fatigue damage model of composite materials. International Journal of Fatigue 2010;32(1):134 – 138. doi:\bibinfo{doi}{http://dx.doi.org/10.1016/j.ijfatigue.2009.02.027}. Fourth International Conference on Fatigue of Composites (ICFC4); URL http://www.sciencedirect.com/science/article/pii/S0142112309000747.

[34] Brinson, H.F.. Matrix dominated time dependent failure predictions in polymer matrix composites. Composite Structures 1999;47(14):445 – 456. doi:\bibinfo{doi}{http://dx.doi.org/10.1016/S0263-8223(00)00075-1}. Tenth International Conference on Composite Structures; URL http://www.sciencedirect.com/science/article/pii/S0263822300000751.

[35] Gamstedt, E., Talreja, R.. Fatigue damage mechanisms in unidirectional carbon-fibre-reinforced plastics. Journal of Materials Science 1999;34(11):2535–2546. doi:\bibinfo{doi}{10.1023/A:1004684228765}. URL http://dx.doi.org/10.1023/A%3A1004684228765.